JP3J.14 HIGH-RESOLUTION SURFACE AND TOWER OBSERVATIONS OF THE SOUTHERN PLAINS DRYLINE DURING PROJECT SONDE-2005

Christopher C. Weiss*
Texas Tech University, Lubbock, Texas

1. INTRODUCTION

Drylines have long been known to be associated with the development of deep convection, owing to the boundary-layer wind convergence accompanying these boundaries. Considering the environments in which drylines are often found (e.g., substantial CAPE and vertical wind shear), subsequent convective development often attains supercellular attributes, with the attendant threat of large hail, damaging winds, and tornadoes. Consequently, the correct prediction of the development of, motion of, and convective initiation along, drylines is imperative to improve the forecasting skill of severe weather hazards.

Previous investigators have provided evidence linking the vertical structure of drylines and the propensity for convective development (e.g., Ziegler and Rasmussen 1998; Peckham and Wicker 2000). As such, observations of the vertical dryline structure are needed in the context of convective development. Since the spatial and temporal scales of variability in the near-dryline environment can be quite diminutive (e.g., Demoz et al. 2005, Weiss et al. 2005), thorough and rapid sampling is desired.

The Simultaneous Observations of the Near-Dryline Environment (SONDE) Project commenced in the southern high Plains on 1 April 2005. The central charge of this ongoing project is, through the diverse and concentrated sampling of the near-dryline environment, to resolve the processes responsible for dryline development and motion. Further, environmental cues for the successful development of sustained deep convection are sought.

Section 2 will include details of the instrumentation used for SONDE-2005. Preliminary results will follow in section 3. A summary and conclusions, and a description of ongoing efforts will be presented in sections 4 and 5, respectively.

* *Corresponding author address: Christopher C. Weiss, Texas Tech University, Atmospheric Science Group, Department of Geosciences, Lubbock, TX, 79409; e-mail: Chris.Weiss@ttu.edu*

2. PROJECT SONDE

Numerous instrument platforms were incorporated for SONDE-2005, including:

Mobile mesonets (FIG. 1) – Four vehicle-mounted instrument racks sampling air temperature, dewpoint temperature, wind direction, wind speed, and barometric pressure at 0.5 Hz.

University of Massachusetts (UMass) W-band radar (FIG. 1) – A 95-GHz mobile Doppler radar used for clear-air sampling (e.g., Weiss et al. 2005). The narrow half-power beamwidth (0.18 deg) permits very-fine spatial resolution.

FIG. 1 – A photograph of the UMass W-band radar (left) and a mobile mesonet probe (right) shortly before dryline transects on 7 May 2005

200 m tower – Located at Reese Technology Center in Lubbock, TX, this tower samples (at 10 Hz) standard meteorological variables at ten vertical levels from the surface up to 200 m AGL.

Vaisala sounding system – A fixed-site radiosonde platform located at Reese Technology Center.

West Texas Mesonet – 45 instrumented stations distributed across the Texas panhandle, with an average inter-station spacing of 50 km.

10 m tower array – Nine fixed-site towers arrayed north-south and east-west, with an average station

spacing of 60 m. Meteorological variables sampled (10 Hz) at 10 m AGL.

There were a total of twelve SONDE case days in spring 2005 (Table 1), allowing for numerous samples of the kinematics and thermodynamics of forward-propagating and retreating drylines. All data collection took place in the Texas panhandle.

3. PRELIMINARY RESULTS (7 MAY 2005)

Surface observations and radar reflectivity data confirm the development of a dryline in the eastern Texas panhandle by 1900 UTC (FIG. 2). Cumulus clouds were widespread along the boundary (FIG. 3). Though towering convection was noted on occasion, no sustained deep convection developed in the vicinity of SONDE operations, perhaps due to the increase of cirrus cloud cover through the afternoon. Convective initiation did occur near the SONDE domain at 2115 UTC (see below), but the updraft quickly dissipated once it had moved away from the dryline.

Mobile mesonet data collection began at 1940 UTC approximately 8 km to the north of Groom, TX. Each probe was responsible for east-west transects of varying lengths. Probe 3 performed 18 transects of the dryline convergence zone through the afternoon. The dewpoint temperature gradient increased steadily from 1.36 ^{o}C / 100 m at 1947 UTC to 3.33 ^{O}C / 100 m at 2315 UTC. Though the dewpoint temperature change was predominantly monotonic, five of the traverses featured a localized reversal of the dewpoint gradient in the dryline zone (FIG. 4). Furthermore, clear depressions in dewpoint temperature were evident approximately 1-2 km east of the primary dewpoint gradient on five traverses (not shown). These features are broadly consistent with regions of subsidence identified in airborne-Doppler dryline observations (e.g., Atkins et al. 1998; Weiss et al. 2002). Such concentrated areas of descent may owe their existence to the vertical wind shear across the dryline interface, similar to the microfronts of Zielger et al. (1995) and the "downdraft hypothesis" of Crawford and Blutestein (1997).

At 2115 UTC, deep convection initiated on the dryline very close to the domain of SONDE operations (FIG. 5). This convection quickly dissipated as it moved away from the dryline. Mobile mesonet traverses before and during initiation were examined for differences in kinematic and thermodynamic properties. Beginning with 2042 UTC, and continuing through the period of initiation, all dewpoint temperature profiles show the aforementioned gradient reversal in the middle of the dryline zone (Figs. 4b-4e), resembling perhaps an "intrusion" of drier air, presumably from above the sloping dryline interface. Coincident with the dry intrusion was a small increase in air temperature, which, assuming conservation of potential temperature and a well-mixed CBL, suggests the source region for the air at the surface was from just above the moist CBL. The magnitude of the temperature increase varied from 0.2 – 1.0 ^{o}C, and was generally located at, and to the west of, the dry intrusion (e.g., FIG. 6).

The diurnal cycle of the dryline favors "forward" eastward progression through the afternoon hours, followed by a westward retrogression beginning in the early evening hours.

Date	West Texas Mesonet	200 m tower (Lubbock)	Tower array (Lubbock)	Mobile mesonet	UMass radar
4/4/05	X	X			
4/9/05	X	X			
4/18/05	X	X			
4/19/05	X	X	X		
4/20/05	X	X	X		
5/7/05	X	X		X	X
5/12/05	X	X	X		
5/13/05	X	X	X		
5/17/05	X	X	X	X	
5/18/05	X	X			
6/11/05	X	X			
6/12/05	X	X	X	X	

Table 1 – Dates and data availability for SONDE-2005 cases

The 7 May 2005 case followed this expected behavior, and dryline retrogression began at approximately 2230 UTC (FIG. 7). The UMass 95-GHz radar joined one mobile mesonet probe in four traverses of the dryline, two before retrogression (2219-2223 UTC and 2225-2234 UTC), and two after retrogression commenced (2257-2304 UTC and 2306-2328 UTC).

Comparison of mobile mesonet traces reveales a sharp increase in the temperature gradient across the dryline as retrogression began, from approximately 0.25 ^{o}C km^{-1} (2219-2223 UTC) to 0.7 ^{o}C km^{-1} (2306-2328 UTC) (FIG. 8). The latter measurement was by far the strongest temperature gradient observed on the dryline up to that time. There were no subsequent traverses to confirm any further increase in the temperature gradient. The virtual temperature gradient across the boundary increased from 0.36 ^{o}C / 2.3 km (pointed eastward) (2219-2223 UTC) to 0.49 ^{o}C / 1.4 km (pointed westward) (2306-2328 UTC). The correlation of the temperature gradient increase to the onset of dryline retrogression supports at least a partial contribution of density-current dynamics to the observed motion (Parsons et al. 1991).

UMass vertical velocity data, obtained with the antenna pointed vertically and transported across the dryline, indicate a maximum upward vertical velocity of 5 m s^{-1} in the dryline convergence zone (FIG. 9). The boundary was steeply sloped in the lowest 1 km AGL, then bended sharply towards the east above 1 km AGL. A concentrated area of subsidence is noted 3-4 km east of the surface dryline position. Downward vertical velocity approached 3 m s^{-1} in the upper portion of the CBL. However, this descending motion extended down to only 500 m AGL, not to the surface. The author speculates that these regions of descent may indeed reach the surface where local dewpoint minima are observed (e.g., FIG. 4). Future coordinated mobile mesonet / UMass radar deployments are needed to confirm this relationship.

4. SUMMARY AND CONCLUSIONS

Dryline transect data from one SONDE case are presented. Mobile mesonet data reveal a clear sharpening of the dryline dewpoint gradient through the afternoon hours.

Beginning approximately one half-hour before convective initation, evidence of an intrusion of dry air becomes apparent in the dryline zone. Coincident small temperature increases suggest that air was subsiding from just above the moist CBL in, and to the west, of the dry intrustion. Such motions may be responsible for the vertical transport of westerly momentum into the boundary layer, thereby enhacing convergence.

Mobile-mesonet data indicate that the dryline assumed a fundamentally different structure at the beginning of retrogression, especially with regards to the temperature gradient across the dryline, which increased substantially.

Mobile Doppler radar data confirm descending motion to the east of the dryline convergence zone, which, when reaching the surface, may relate to the observed local dewpoint minima.

5. ONGOING WORK

Analysis is ongoing on the presented SONDE case to integrate mobile-mesonet wind observations and better delineate the evolution of dryline convergence. Data from the other three probes will be incorporated to confirm or refute the findings presented here.

Other SONDE cases will also be thoroughly investigated, most of which include tower data. The vertical structure of the forward-passing and retreating dryline will be analyzed in detail.

Results from this ongoing work will be presented at the conference.

6. ACKNOWLEDGEMENTS

The author is grateful to the Texas Tech Wind Science and Engineering Center for the support and facilities to carry out this ongoing research. Also, thanks to the faculty and students in the Atmospheric Science Group at Texas Tech, the Wind Science and Engineering IGERT program, the School of Meteorology at the University of Oklahoma, and the Microwave Remote Sensing Laboratory at the University of Massachusetts-Amherst who provided resources and assisted in the data collection, particularly Howie Bluestein, Steve Frasier, John Schroeder, Eric Holthaus, Pei-Sang Tsai, and Robin Tanamachi. Ian Giammanco and Brian Hirth were instrumental in preparing and calibrating the mobile mesonet racks.

7. REFERENCES

Atkins, N. T., R. M. Wakimoto, and C. L. Ziegler, 1998: Observations of the finescale structure of a dryline during VORTEX-95: *Mon. Wea. Rev.*, **126**, 525-550.

Crawford, T. M., and H. B. Bluestein, 1997: Characteristics of dryline passage. *Mon. Wea. Rev.*, **125**, 463-477.

Demoz, B., and Coauthors, 2005: The dryline on 22 May 2002 during IHOP_2002: Convective scale measurements at the profiling site. *Mon. Wea. Rev.* (accepted)

Parsons, D. B., M. A. Shapiro, R. M. Hardesty, R. J. Zamora, and J. M. Intrieri, 1991: The finescale structure of a west Texas dryline. *Mon. Wea. Rev.*, **119**, 1283-1292.

Peckham, S. E., and L. J. Wicker, 2000: The influence of topography and lower-tropospheric winds on dryline morphology. *Mon. Wea. Rev.*, **128**, 2165-2189.

Weiss, C. C., and H. B. Bluestein, 2002: Airborne pseudo-dual Doppler analysis of a dryline-outflow boundary intersection. *Mon. Wea. Rev.*, **130**, 1207-1226.

——, ——, and A. L. Pazmany, 2005: Fine-scale radar observations of the 22 May 2002 dryline during the International H_2O Project (IHOP). *Mon. Wea. Rev.* (accepted)

Ziegler, C. L., and E. N. Rasmussen, 1998: The initiation of moist convection at the dryline: Forecasting issues from a case study perspective. *Wea. Forecasting*, **13**, 1106-1131.

——, W. J. Martin, R. A. Pielke, and R. L. Walko, 1995: A modeling study of the dryline. *J. Atmos. Sci.*, **52**, 263-285.

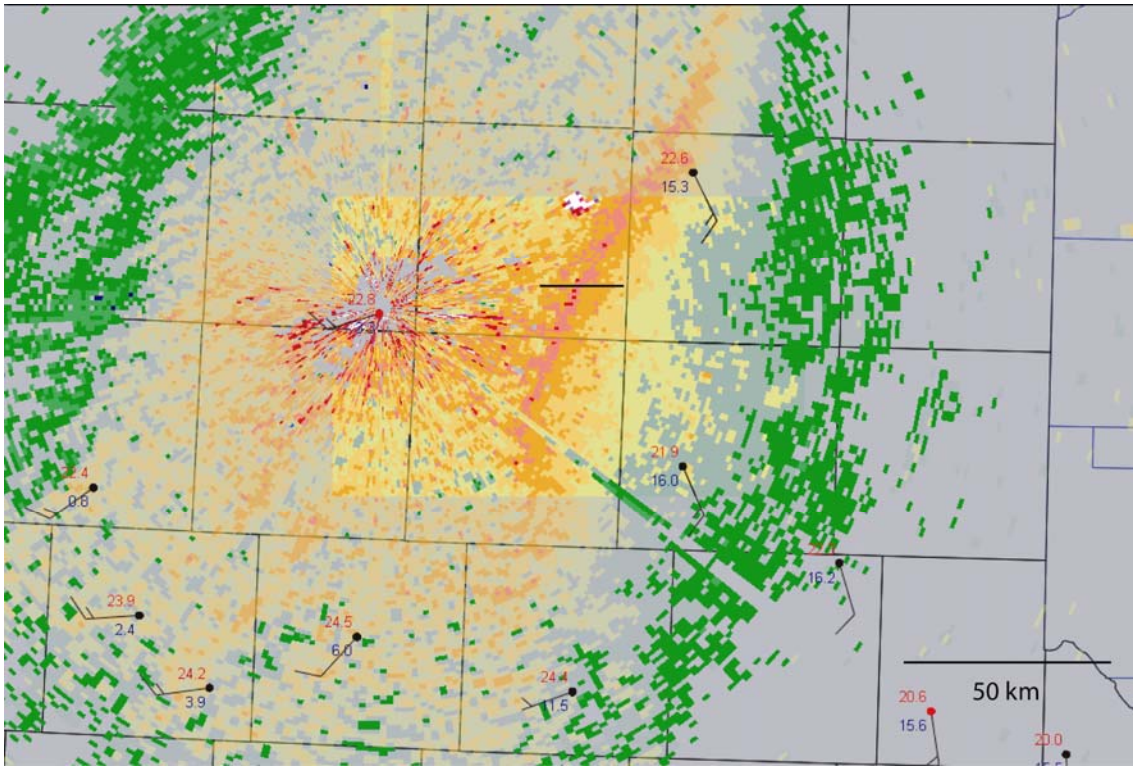

FIG. 2 – 0.5 deg reflectivity from the Amarillo, TX WSR-88D (KAMA) at 1905 UTC on 7 May 2005. The black line represents the domain of SONDE operations. The echo directly to the north of the black line is a ground target. Distance scale is provided in the lower right hand corner.

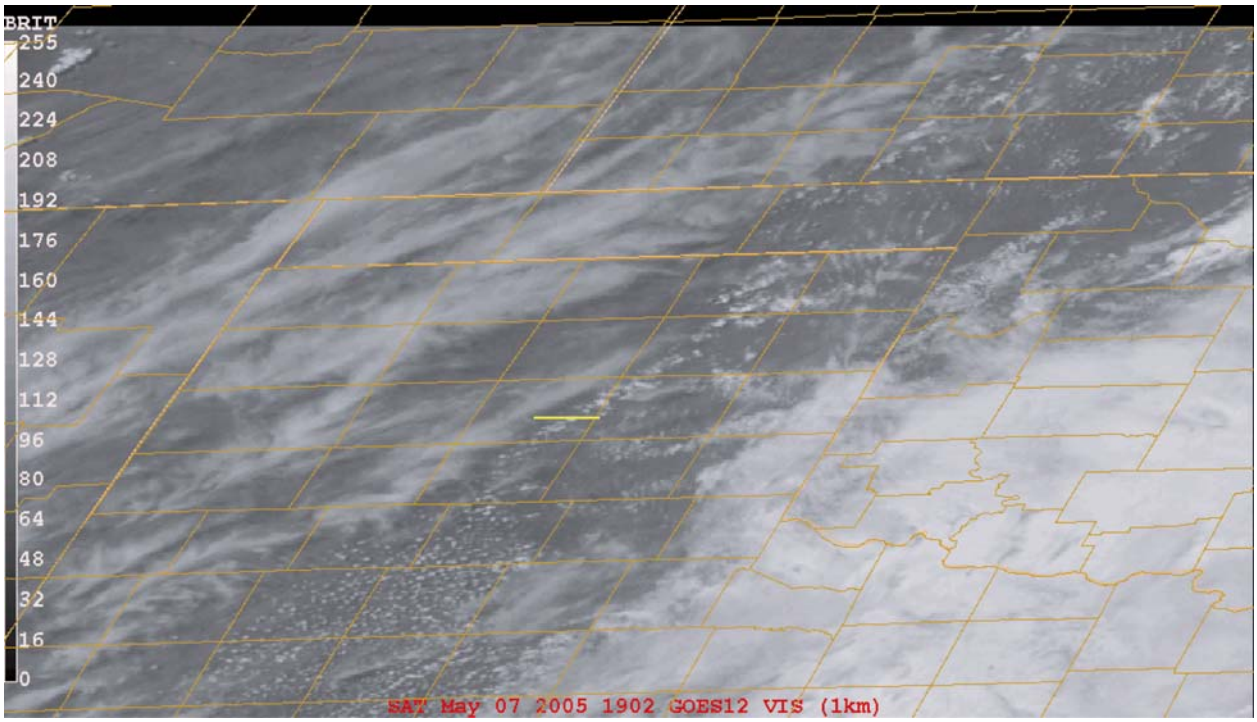

FIG. 3 – GOES-12 visible satellite image valid at 1902 UTC on 7 May 2005. The yellow line represents the domain of SONDE operations.

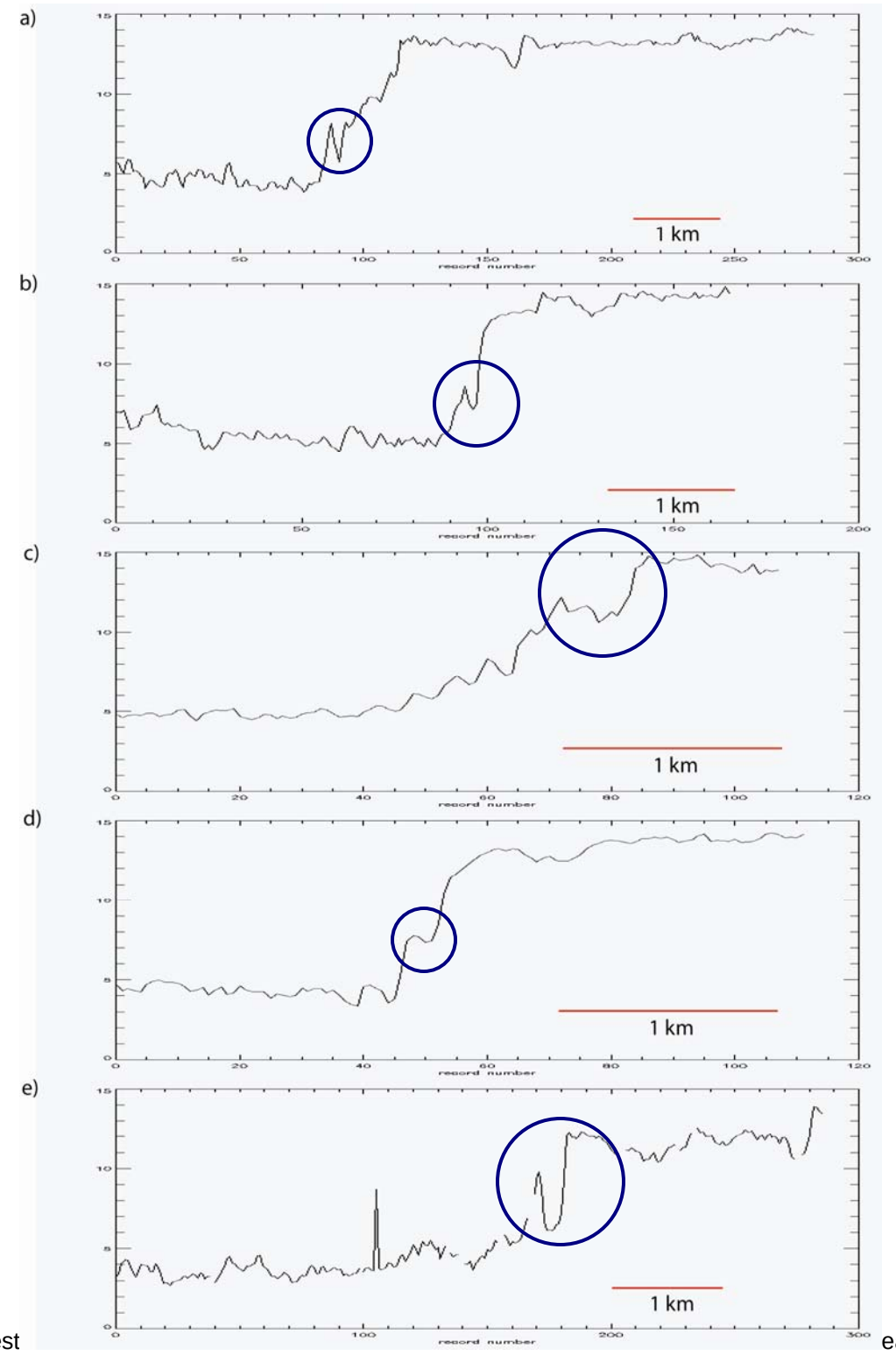

FIG. 4 – Traces of mobile-mesonet-measured dewpoint temperature (^{o}C) from a) 2004-2014 UTC, b) 2042-2048 UTC, c) 2048-2052 UTC, d) 2052-2056 UTC, and e) 2100-2110 UTC. Scales for 1 km are indicated by the red line. Regions of dewpoint gradient reversal are circled in each panel.

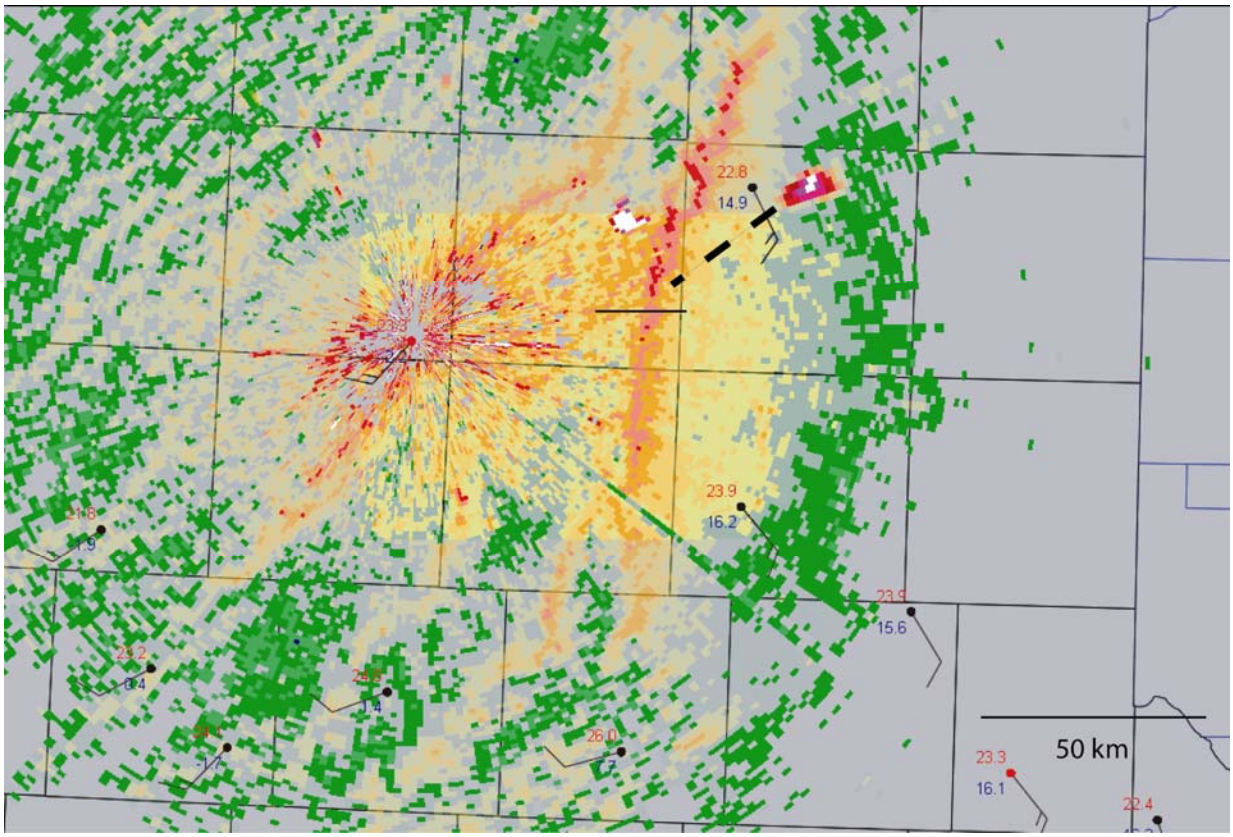

FIG. 5 – As in FIG. 2, but valid at 2155 UTC. The dashed line traces the previous path of the convective development (including the period before first echo).

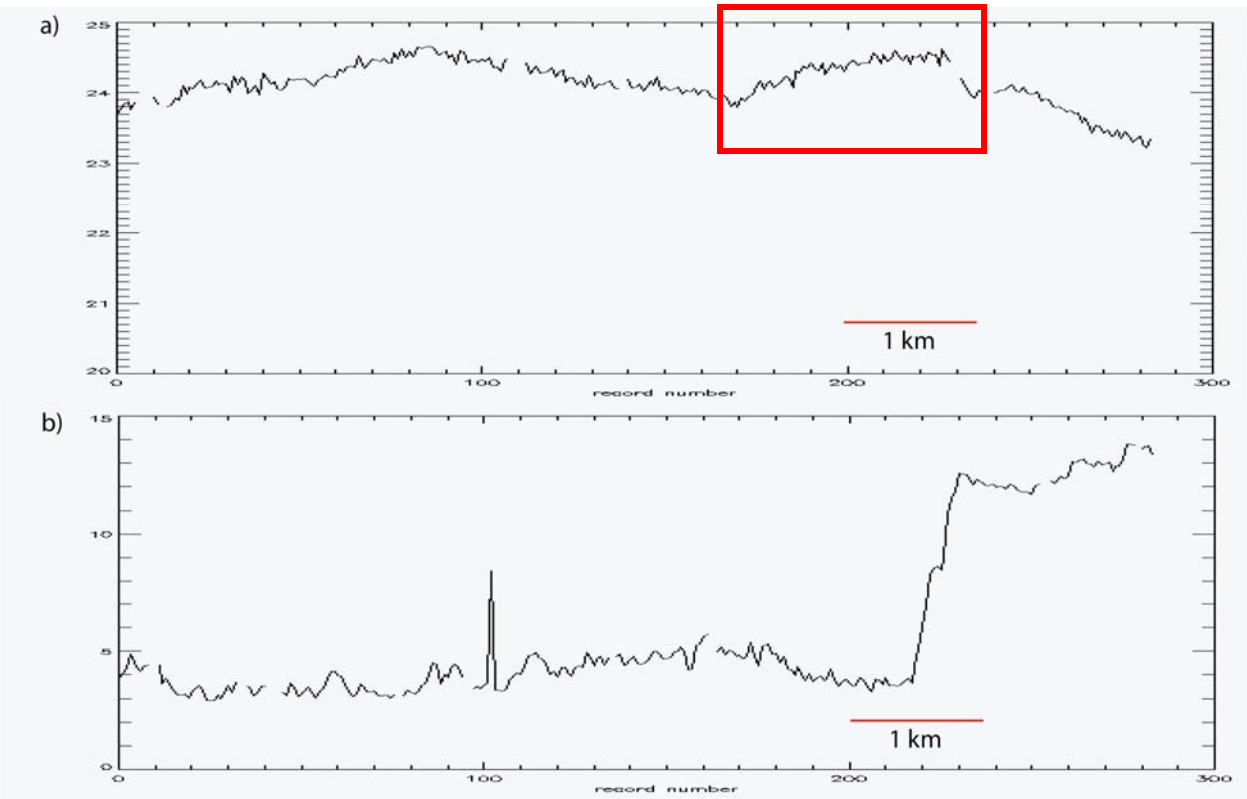

west *east*

FIG. 6 – Mobile mesonet traces of a) air temperature (°C) and b) dewpoint temperature (°C) from 2110-2120 UTC. 1 km scales are indicated by the red line. The red box denotes the maximum in air temperature to the west of the dryline zone.

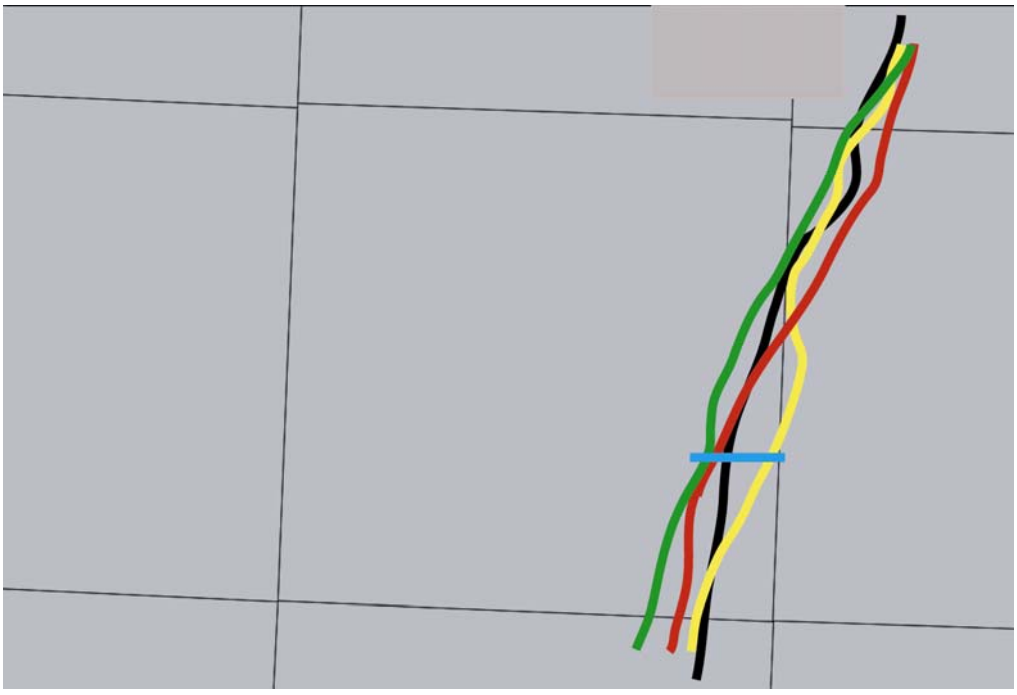

FIG. 7 – Isochrones of dryline position on 7 May 2005 at 2200 UTC (black), 2230 UTC (yellow), 2300 UTC (red), and 2330 UTC (green). The blue line denotes the domain of SONDE operations.

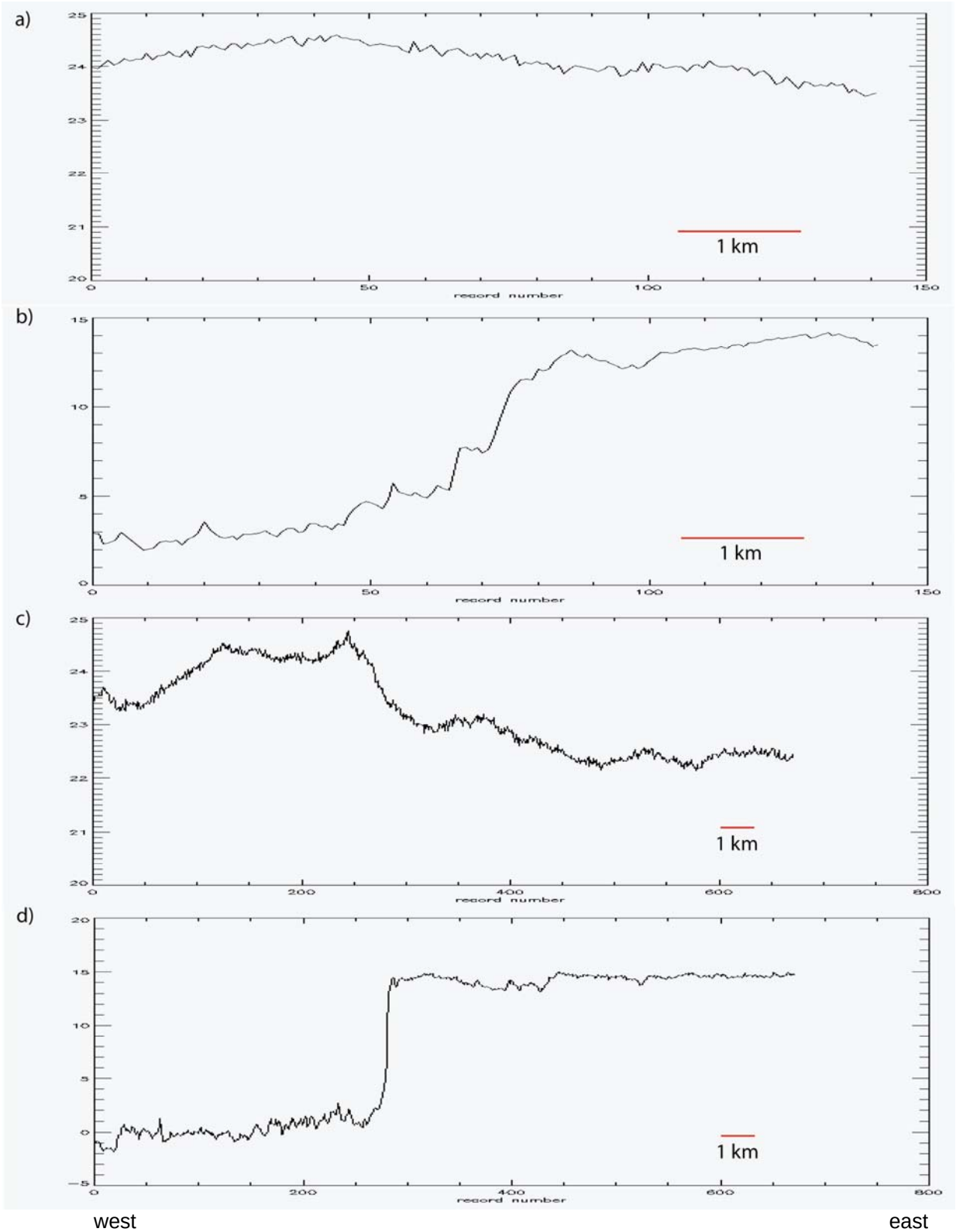

FIG. 8 – Mobile mesonet traces of a) air temperature (^{o}C) and b) dewpoint temperature (^{o}C) from 2219-2223 UTC; c) and d) same as a) and b), except from 2306-2328 UTC. 1 km scales are indicated by the red line.

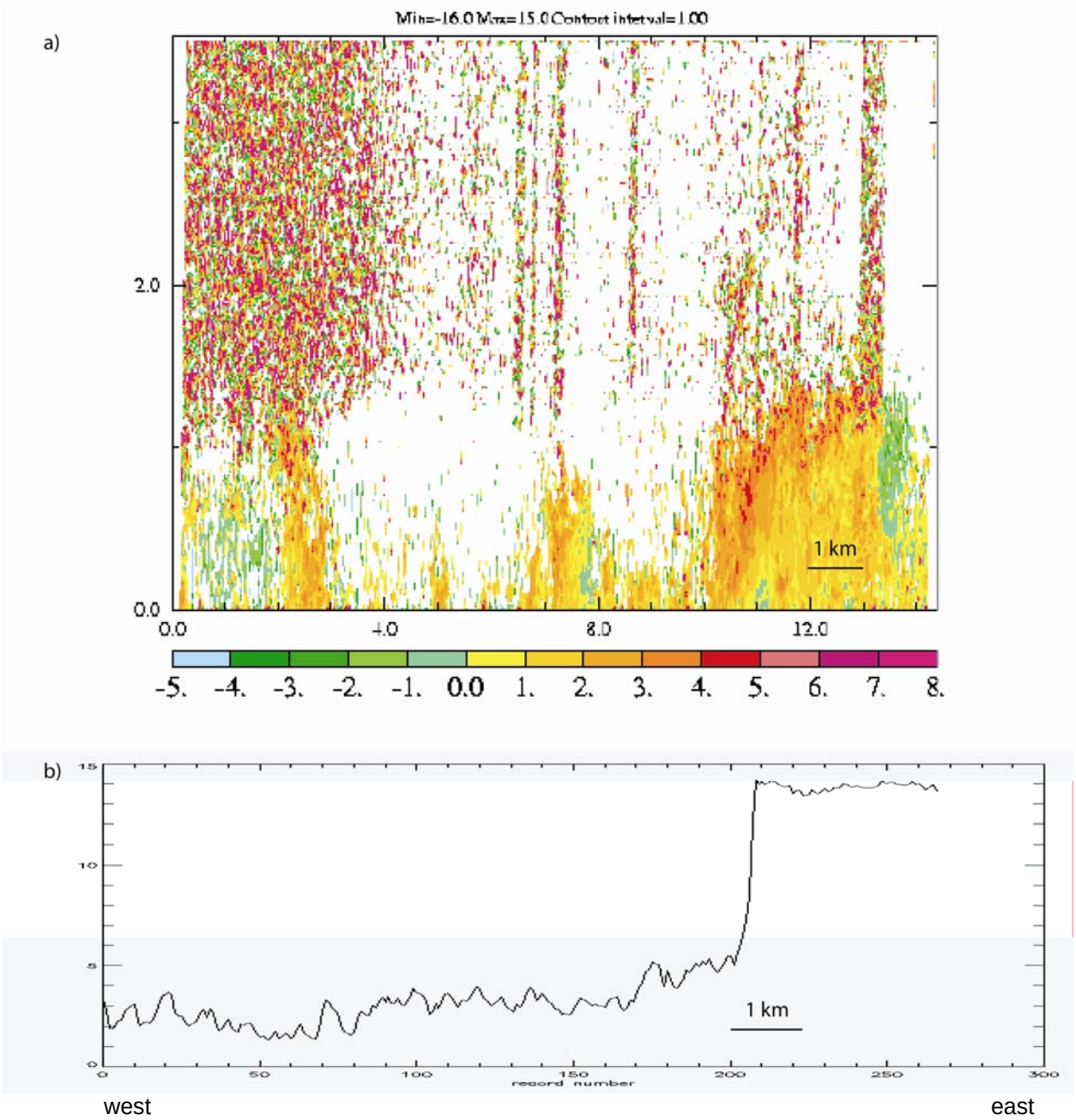

FIG. 9 – a) Vertical velocity (m s^{-1}) data obtained from 2225-2234 UTC with the UMass 95-GHz radar. The velocity scale is shown at the bottom; b) Mobile mesonet dewpoint temperature (^{o}C) trace valid for approximately the same time as a). 1 km distance scales are provided at the bottom of each panel.